

Gravitational wave fluxes on generic orbits in near-extreme Kerr spacetime: higher spin and large eccentricity

Changkai Chen,^{}^a Jiliang Jing,^{}^{a,1}

^aDepartment of Physics, Key Laboratory of Low Dimensional Quantum Structures and Quantum Control of Ministry of Education, Synergetic Innovation Center for Quantum Effects and Applications, Hunan Normal University, Changsha, 410081, Hunan, China

E-mail: chenck@hunnu.edu.cn, jljing@hunnu.edu.cn

ABSTRACT: To obtain the waveform template of gravitational waves (GWs), substantial computational resources and exceedingly high precision are often required. In the previous study [[JCAP 11 \(2023\) 070](#)], we efficiently and accurately calculate GW fluxes of a particle in circular orbits around a Schwarzschild black hole using the confluent Heun function. We extend the previous method to calculate the asymptotic GW fluxes from a particle in generic orbits around a near-extreme Kerr black hole. Especially when dealing with the computational difficulties in large eccentricity $e = 0.9$, higher spin $a = 0.999$, higher harmonic modes, and strong-field regions, our results are much better than the results of the numerical integration method based on the Mano-Suzuki-Takasugi method.

KEYWORDS: Black Holes, Classical Theories of Gravity

ARXIV EPRINT: [2311.15295](#)

¹Corresponding author.

Contents

1	Introduction	1
2	Kerr geodesics	4
2.1	Formulations of orbital frequencies	4
2.2	Orbit parameterization and initial conditions	5
3	GW Radiative Fluxes via the Teukolsky equation	6
3.1	Exact Solutions of Teukolsky equations	6
3.2	Radiative Fluxes	9
4	Comparisons with other methods	11
5	Conclusion	15
A	Formulas for E, L_z, and Q	16
B	Asymptotic Formula of HeunC Function at Infinity	17
C	Parameters of HeunC Functions	18

1 Introduction

The two-body problem holds a crucial position in general relativity. It has garnered significant attention in the field of GW astronomy due to the potential of binary black hole (BBH) inspirals to generate GWs, which are expected to be detected directly by ongoing GW observatories worldwide [1–5]. Future space-based GW detectors, such as the Laser Interferometer Space Antenna (LISA) [6, 7], TianQin [8, 9], and Taiji [10], will be built with the specific purpose of detecting GW signals from sources that radiate in the millihertz bandwidth, namely extreme mass ratio inspirals (EMRIs). EMRI events enable the precise mapping of black hole (BH) spacetimes, allowing for the accurate determination of BH masses and spins. This offers an opportunity to test the hypothesis that astrophysical BHs conform to Kerr spacetime [11]. To comprehend the dynamics of BBHs, accurately predicting GW waveforms is essential for effectively detecting signals in observed data.

A primary approach to achieve this purpose is calculations of gravitational self-force (GSF) within black hole perturbation (BHP) theory. The system of BBHs is considered as a point mass orbiting a black hole, and its dynamics can be described by the equation of motion that includes the effect of the interaction with its self-field, known as the GSF. The formalism of GSF calculations was initially established by Mino, Sasaki, and Tanaka in the mid-1990s [12], along with Quinn and Wald [13]. Over the past two decades, this formalism has seen significant refinement to improve

both its mathematical rigor and conceptual clarity. For comprehensive reviews and further research on the GSF, please refer to Refs. [14–18].

One commonly employed approach to compute the GSF involves utilizing the Weyl scalars ψ_0 and ψ_4 that satisfy the separable Teukolsky equation [19–22]. These scalars contain the majority of the gauge invariant information regarding the complete metric perturbation [23]. In the 1970s, Chrzanowski, Cohen, and Kegeles (CCK) [24–26] developed a method to reconstruct vacuum metric perturbations in a radiation gauge from vacuum solutions of ψ_0 and ψ_4 . However, as Ori pointed out [27], when this method is applied to the field generated by a point particle source, the resulting metric perturbation becomes highly singular. The singularities in the metric perturbation are not only found at the position of the particle, but also manifest as a stringlike gauge singularity that extends from the particle to the event horizon or infinity. It is uncertain whether the established GSF form can be extended to account for this type of singularity. Subsequently, Pound et al. [28] discovered that the GSF can be extracted from the metric perturbations in the radiation gauge. Friedman’s group [29–31] pioneered the radiation gauge method of the GSF, and they calculated the Detweiler redshift invariance on the circular equatorial orbit of the Kerr spacetime [32]. Maarten extended their method to calculate the first-order GSF and redshifts on eccentric equatorial orbits [33, 34] and generic bound orbits [35] (featuring both eccentricity and inclination). Furthermore, while ψ_0 or ψ_4 carry most of the information regarding metric perturbations, the perturbations of “mass” and “angular momentum” must be recovered through alternative methods [23]. Merlin et al. [36] reconstructed these components for fields sourced by a particle in equatorial orbits by imposing the continuity of certain gauge-invariant fields derived from the metric. The results are characterized by simplicity: Outside the particle’s orbit, the mass and angular momentum perturbations are solely determined by the orbital energy and orbital angular momentum, while both perturbations vanish within the orbit. Using the direct method of metric perturbation generated by the CCK procedure, it is demonstrated that this result is indeed applicable to any compact source in the radial direction [37].

Much progress has been achieved in calculating the GSF for various orbits, but it remains particularly challenging for generic orbits, especially in Kerr spacetime. Three fundamental frequencies $\Omega_{r,\theta,\phi}$ characterize the generic geodesic orbits. However, calculating these frequencies is considerably difficult, and no efficient and accurate method for the GSF calculations of generic orbits has been developed thus far. Due to the regularization problem of the point mass limit, high-precision GSF requires magnanimous computational cost in practical calculations. Therefore, it is very crucial to study a method to reduce the computational cost of GSF. The two-timescale expansion method [38] provides a hint: assuming that a point mass does not encounter any transient resonance [39], the orbital phase is the most significant information for the prediction of the GW waveform, which can be written as

$$\Phi = \epsilon^{-1} \left[\Phi^{(0)} + \epsilon \Phi^{(1)} + O(\epsilon^2) \right], \quad (1.1)$$

where the mass ratio $\epsilon = m_2/m_1 \leq 1$. And the leading-order term $\Phi^{(0)}$ can be considered as the time-averaged dissipative effect of the first-order GSF. The calculation of this secular effect can be simplified by defining the radiative field as half of the retarded solution of the gravitational perturbation equation minus half of the advanced solution, using the adiabatic approximation method [40, 41]. This is effective because the radiative field is a homogeneous solution of the divergence

that is induced by the point mass limit. By using this method, the leading-order term can be accurately calculated without huge computational cost. On the other hand, $\Phi^{(1)}$ corresponds to the residual part of the first-order GSF, which includes the oscillatory part of both the dissipative and conservative GSFs, as well as the time-averaged dissipative part of the second-order GSF. Currently, there is no simplified approach available to calculate these post-adiabatic components accurately. However, since $\Phi^{(1)}$ is considered a minor factor, the requirement for precision is not stringent. This fact suggests that the computational burden can be reduced by employing suitable methods with appropriate error tolerance to compute each piece of the GSF. Based on this formalism, Osburn et al. proposed a hybrid scheme for calculating the GSF of eccentric orbits [42].

For non-spinning particles in generic orbits around a Kerr BH, the time-averaged dissipative part of the first-order GSF is the dominant contribution to the inspiral evolution in Kerr spacetime, making it suitable for calculating GW fluxes necessary for constructing GW waveforms. By using the Teukolsky equation to calculate the dissipative first-order GSF, there have been some breakthroughs. Hughes successfully solved the short-range potential form ¹ (Sasaki-Nakamura equation) of the Teukolsky equation by numerical integration [44], and provide the inspiral evolution and snapshot waveforms for spherical orbits (circular and nonequatorial) in Kerr spacetime [45]. Based on the frequency-domain orbit function of Kerr BHs [46], his group extended the GSF to generic orbits [47]. After years of research, his group also gave a long inspiral waveform of EMRIs in generic orbits [48]. Moreover, they calculated the EMRI waveforms [49] of a spinning body moving on generic orbits in the second-order spin by using the frequency-domain method proposed in Refs. [50, 51]. Fujita’s group from Japan first used the Mano-Suzuki-Takasugi (MST) method to give an efficient numerical method for calculating the dissipative GSF of generic orbits [52]. Then, based on the MST method and the analytical solution of bound timelike geodesic orbits in Kerr spacetime [53], they derived the analytical formula of high-order post-Newtonian (PN) expansion [54]. They used this analytical formula to study the measurability of EMRI waves by LISA, and their discussion was mainly about the adiabatic waveforms of eccentric and equatorial sources [55]. Their numerical and analytical methods are widely used in the construction of waveforms with any mass ratio [56, 57]. The results of these two teams have excellent computational performance. Their methods can not only calculate the dissipative GSF of generic orbits in Kerr spacetime with large eccentricities, large inclinations, high harmonic modes, and strong-field regions, but also exhibit extremely high computational accuracy. Other EMRI waveforms or GSF calculations can only calculate small eccentricity ($e \leq 0.3$) or Schwarzschild BHs [35, 58, 59]. Our previous study [60] proposed an exact approach to calculate GW fluxes from a particle in circular orbits around a Schwarzschild BH using the confluent Heun function. The computational accuracy and efficiency of this exact approach are comparable to those of the MST method and the numerical integration method.

In this work, *we extend the previous work to obtain GW radiative fluxes from a particle in generic orbits around a Kerr BH.* We aim to compute and store the grid data of radiative fluxes so that it can cover the extreme cases of orbital parameters: $a = 0.999$, $e = 0.9$, large inclinations and high harmonic modes. This work will provide an accurate and efficient choice of energy flux data

¹Sasaki and Nakamura gave a transformation [43], which converts the Teukolsky function $R(r)$ governed by an equation with long-range potential into the Sasaki-Nakamura function $X(r)$ governed by an equation with short-range potential.

and GW amplitudes for waveform construction.

The remainder of the paper is arranged as follows. Section 2 provide a brief review of the geodesic motion of a point particle in Kerr spacetime. In Section 3, we give the exact solution of the Teukolsky equation of the Kerr BH in the form of the confluent Heun function, which is used to calculate the radiative energy fluxes on the generic orbit. Section 4 is devoted to comparing our results with those of PN expansion and the MST methods to validate the high precision of our approach. Finally, the conclusion of this paper is presented in Section 5, which includes plans and directions for future work. In this paper, we use geometrized units: $c = G = 1$.

2 Kerr geodesics

In this section, we discuss bounded Kerr geodesics. The detailed content can be seen in Refs.[46–48, 53, 54, 61, 62], we briefly review the geodesic dynamics of a point particle in the Kerr spacetime. Some lengthy but important formulas are given in Appendix A.

Firstly, the Kerr metric in the Boyer-Lindquist coordinates, (t, r, θ, φ) , can be given by

$$g_{\mu\nu}dx^\mu dx^\nu = -\left(1 - \frac{2Mr}{\Sigma}\right)dt^2 - \frac{4Mar \sin^2 \theta}{\Sigma}dt d\varphi + \frac{\Sigma}{\Delta}dr^2 + \Sigma d\theta^2 + \left(r^2 + a^2 + \frac{2Ma^2r}{\Sigma} \sin^2 \theta\right) \sin^2 \theta d\varphi^2, \quad (2.1)$$

where $\Sigma = r^2 + a^2 \cos^2 \theta$, $\Delta = (r - r_-)(r - r_+)$ and $r_\pm = M \pm \sqrt{M^2 - a^2}$. r_- is the inner horizon, and r_+ is the outer (event) horizon. Here, M and aM are the mass and angular momentum of the Kerr BH, respectively.

2.1 Formulations of orbital frequencies

We use Mino time as our time parameter to describe these bound orbits [48, 53]. An interval of Mino time $d\lambda$ is related to an interval of proper time $d\tau$ by $d\lambda = d\tau/\Sigma$, the geodesic equations become

$$\left(\frac{dr}{d\lambda}\right)^2 = [E(r^2 + a^2) - aL_z]^2 - \Delta[r^2 + (L_z - aE)^2 + Q] \equiv R(r), \quad (2.2)$$

$$\left(\frac{d\theta}{d\lambda}\right)^2 = Q - \cot^2 \theta L_z^2 - a^2 \cos^2 \theta (1 - E^2) \equiv \Theta(\theta), \quad (2.3)$$

$$\frac{d\phi}{d\lambda} = \csc^2 \theta L_z + \frac{2MraE}{\Delta} - \frac{a^2 L_z}{\Delta} \equiv \Phi_r(r) + \Phi_\theta(\theta), \quad (2.4)$$

$$\frac{dt}{d\lambda} = E \left[\frac{(r^2 + a^2)^2}{\Delta} - a^2 \sin^2 \theta \right] - \frac{2MraL_z}{\Delta} \equiv T_r(r) + T_\theta(\theta). \quad (2.5)$$

where E , L_z , and Q are the orbit's energy (per unit μ), axial angular momentum (per unit μ), and Carter constant (per unit μ^2), respectively. The expressions of these quantities are shown in Eq. (A.1) to (A.3).

It can be seen from Eqs. (2.2) and (2.3) that the bound orbit of the radial and the polar motion is periodic when parameterized using λ :

$$r(\lambda) = r(\lambda + n\Lambda_r), \quad \theta(\lambda) = \theta(\lambda + k\Lambda_\theta), \quad (2.6)$$

where n and k are integers. For fundamental periods $\Lambda_{r,\theta,\phi}$, we can define the associated frequencies: $\Upsilon_{r,\theta,\phi} = 2\pi/\Lambda_{r,\theta,\phi}$. The orbital motions in t and ϕ is the sum of the long-term cumulative part and oscillation functions:

$$t(\lambda) = t_0 + \Upsilon_t \lambda + \Delta t_r[r(\lambda)] + \Delta t_\theta[\theta(\lambda)] , \quad (2.7)$$

$$\phi(\lambda) = \phi_0 + \Upsilon_\phi \lambda + \Delta \phi_r[r(\lambda)] + \Delta \phi_\theta[\theta(\lambda)] . \quad (2.8)$$

where t_0 and ϕ_0 describe initial conditions,

$$\Upsilon_t = \langle T_r(r) \rangle + \langle T_\theta(\theta) \rangle , \quad \Upsilon_\phi = \langle \Phi_r(r) \rangle + \langle \Phi_\theta(\theta) \rangle , \quad (2.9)$$

$$\Delta t_r[r(\lambda)] = T_r[r(\lambda)] - \langle T_r(r) \rangle \equiv \Delta t_r(\lambda) , \quad \Delta t_\theta[\theta(\lambda)] = T_\theta[\theta(\lambda)] - \langle T_\theta(\theta) \rangle \equiv \Delta t_\theta(\lambda) , \quad (2.10)$$

$$\Delta \phi_r[r(\lambda)] = \Phi_r[r(\lambda)] - \langle \Phi_r(r) \rangle \equiv \Delta \phi_r(\lambda) , \quad \Delta \phi_\theta[\theta(\lambda)] = \Phi_\theta[\theta(\lambda)] - \langle \Phi_\theta(\theta) \rangle \equiv \Delta \phi_\theta(\lambda) . \quad (2.11)$$

The quantity Υ_t and Υ_ϕ are the frequencies of coordinate time t and ϕ with respect to λ respectively. The averages $\langle T_{r,\theta} \rangle$ and $\langle \Phi_{r,\theta} \rangle$ in Eq. (2.9) to (2.11) are given by

$$\langle T_r(r) \rangle = \frac{1}{\Lambda_r} \int_0^{\Lambda_r} T_r[r(\lambda)] d\lambda , \quad \langle T_\theta(\theta) \rangle = \frac{1}{\Lambda_\theta} \int_0^{\Lambda_\theta} T_\theta[\theta(\lambda)] d\lambda , \quad (2.12)$$

$$\langle \Phi_r(r) \rangle = \frac{1}{\Lambda_r} \int_0^{\Lambda_r} \Phi_r[r(\lambda)] d\lambda , \quad \langle \Phi_\theta(\theta) \rangle = \frac{1}{\Lambda_\theta} \int_0^{\Lambda_\theta} \Phi_\theta[\theta(\lambda)] d\lambda . \quad (2.13)$$

The observer-time frequencies can be written as

$$\Omega_{r,\theta,\phi} = \frac{\Upsilon_{r,\theta,\phi}}{\Upsilon_t} . \quad (2.14)$$

2.2 Orbit parameterization and initial conditions

The orbit ranges of radial and polar motion are set to $\theta_{\min} \leq \theta \leq \theta_{\max}$ and $r_{\min} \leq r \leq r_{\max}$, respectively. Here, $\theta_{\max} = \pi - \theta_{\min}$ and $r_{\min/\max} = p/(1 \pm e)$. In order to avoid ambiguity, we use the inclination angle I instead of θ_{\min} , and their relation is $I = \pi/2 - \text{sgn}(L_z)\theta_{\min}$. Because it can smoothly change from 0 for equatorial prograde to π for equatorial retrograde. The cosine of the inclination angle, $x_I \equiv \cos I$, is an excellent parameter to describe inclination: x_I varies smoothly from 1 to -1 as orbits vary from prograde equatorial to retrograde equatorial, with L_z having the same sign as x_I . The generic geodesic orbit in Kerr spacetime can be characterized by three parameters, (E, L_z, Q) . However, for the bound orbit, another set of parameters (p, e, x_I) is chosen for convenience [61, 62].

Eqs. (2.7) and (2.8) can give the initial conditions t_0 and ϕ_0 . To set initial conditions in the r and θ directions, we introduce anomaly angles χ_r and χ_θ to reparameterize these coordinate motions.

$$r = \frac{p}{1 + e \cos(\chi_r + \chi_{r0})} , \quad (2.15)$$

$$\cos \theta = \sqrt{1 - x_I^2} \cos(\chi_\theta + \chi_{\theta 0}) . \quad (2.16)$$

We set $\chi_\theta = 0$, $\chi_r = 0$, $t = t_0$, and $\phi = \phi_0$ when $\lambda = 0$. The phase χ_{r0} then determines $r(0)$, and $\chi_{\theta 0}$ determines the corresponding value of θ . When $\chi_{\theta 0} = 0$, the orbit has $\theta = \theta_{\min}$ when $\lambda = 0$; when $\chi_{r0} = 0$, it has $r = r_{\min}$ when $\lambda = 0$.

We define *fiducial geodesic* as the geodesic that has $\chi_{\theta 0} = \chi_{r0} = \phi_0 = 0 = t_0$. The quantity with a ‘‘check-mark’’ indicates that the quantity is along the fiducial geodesic. Such as $\check{r}(\lambda)$ and $\check{\theta}(\lambda)$ are radial and polar directions along the fiducial geodesic.

For non-fiducial geodesics, we introduce definitions: when $r = r_{\min}$, $\lambda_{r0} = \min(\lambda)$; when $\theta = \theta_{\min}$, $\lambda_{\theta 0} = \min(\lambda)$. This means that

$$r(\lambda) = \check{r}(\lambda - \lambda_{r0}), \quad \theta(\lambda) = \check{\theta}(\lambda - \lambda_{\theta 0}), \quad (2.17)$$

These definitions show that these motions are periodic: $r(\lambda_{r0} + n\Lambda_r) = r_{\min}$ for any integer n , and $\theta(\lambda_{\theta 0} + k\Lambda_\theta) = \theta_{\min}$ for any integer k . There is the relations between $\lambda_{\theta 0}$ and $\chi_{\theta 0}$, and between λ_{r0} and χ_{r0} . A useful corollary is

$$\begin{aligned} \Delta t_r(\lambda) &= \Delta \check{t}_r(\lambda - \lambda_{r0}) - \Delta \check{t}_r(-\lambda_{r0}), \\ \Delta t_\theta(\lambda) &= \Delta \check{t}_\theta(\lambda - \lambda_{\theta 0}) - \Delta \check{t}_\theta(-\lambda_{\theta 0}), \end{aligned} \quad (2.18)$$

with analogous formulas for $\Delta\phi_r$ and $\Delta\phi_\theta$.

Many of the definitions in this section are derived from Hughes’ latest review of bound Kerr geodesics [48]. The introduction of these quantities ($\chi_{r0}, \chi_{\theta 0}, \phi_0$) facilitates the calculation of inspiral evolution in the adiabatic approximation.

3 GW Radiative Fluxes via the Teukolsky equation

The next key in constructing adiabatic inspirals is the calculation of the dissipative part of the first-order GSF. It can give the associated gravitational wave amplitude and radiative fluxes. In this section, we extend the previous method [60] to the Kerr spacetime to calculate these quantities.

3.1 Exact Solutions of Teukolsky equations

In the Teukolsky formalism, the gravitational perturbation of a Kerr black hole is described in terms of the null-tetrad component of the Weyl tensors, that is ψ_0 and ψ_4 . These scalars satisfy the master equation [20]. The Weyl scalar Ψ_4 is related to the GW amplitude at infinity as

$$\psi_4 \rightarrow \frac{1}{2}(\ddot{h}_+ - i\ddot{h}_\times), \quad \text{for } r \rightarrow \infty. \quad (3.1)$$

The master equation for ψ_4 can be separated into radial and angular parts if we expand ψ_4 in Fourier harmonic modes as

$$\rho^{-4}\psi_4 = \sum_{\ell m} \int_{-\infty}^{\infty} d\omega e^{-i\omega t + im\varphi} {}_{-2}S_{\ell m}^{a\omega}(\vartheta) R_{\ell m \omega}(r), \quad (3.2)$$

where $\rho = (r - ia \cos \vartheta)^{-1}$, and the angular function ${}_{-2}S_{\ell m}^{a\omega}(\vartheta)$ is the spin-weighted spheroidal harmonic² with spin $s = -2$. The radial function $R_{\ell m \omega}(r)$ satisfies the radial Teukolsky equation,

$$\left[\Delta^{-s+1} \frac{d}{dr} \Delta^{s+1} \frac{d}{dr} + V(r) \right] R_{\ell m \omega} = \Delta T_{\ell m \omega}, \quad (3.3)$$

²Note the distinction between (θ, ϕ) of the orbits and (ϑ, φ) of the measured field.

and the potential term $V(r)$ is given as

$$V(r) = K^2 - isK\Delta' + \Delta(2isK' - \hat{\lambda}), \quad (3.4)$$

where $K = (r^2 + a^2)\omega - ma$ and $\hat{\lambda}$ is the eigenvalue of ${}_{-2}S_{\ell m}^{a\omega}(\vartheta)$. The computational methods of the angular function ${}_{-2}S_{\ell m}^{a\omega}(\vartheta)$ and the source function $T_{\ell m\omega}$ are discussed in Refs. [44, 63, 64].

The most commonly used methods for solving the homogenous solutions $R_{\ell m\omega}^{\text{in,up}}$ of the Teukolsky equation are the PN expansion [65–68] of the Sasaki-Nakamura equation and the MST method [63, 69, 70]. We presented a exact approach that surpasses the MST method in terms of accuracy for calculating gravitational radiation at the horizon and infinity. The key pieces of our approach have been summarized in depth in the previous paper [60]. Here, we provide a very brief sketch largely to set the context for the following discussion. The general solution of the homogenous form of Eq. (3.3) is derived by the linear combination of two linearly independent particular solutions.

$$R_{\ell m\omega} = C_1 S_0^\beta(x) \text{HeunC}(\alpha, \beta, \gamma, \delta, \eta; x) + C_2 S_0^{-\beta}(x) \text{HeunC}(\alpha, -\beta, \gamma, \delta, \eta; x), \quad (3.5)$$

where C_1 and C_2 are constants that should be determined based on different boundary conditions. Here, HeunC is the confluent Heun function [71–73], and x is defined as a new coordinate that is obtained by applying a Möbius (isomorphic) transformation, which is a linear fractional transformation of the form

$$x = -\frac{r - r_+}{r_+ - r_-}, \quad (3.6)$$

and the unnormalized S-homotopic transformation,

$$S_0^\beta(x) = (-x)^{\frac{1}{2}(\beta-s)}(1-x)^{\frac{1}{2}(\gamma-s)}e^{\frac{1}{2}\alpha x}, \quad (3.7)$$

and the parameters $\alpha, \beta, \gamma, \delta$, and η are given by

$$\alpha = -2i\omega r_x, \quad (3.8a)$$

$$\beta = -s + r_x^{-1} (2i\omega(r_+^2 + a^2) - 2iam), \quad (3.8b)$$

$$\gamma = s + r_x^{-1} (2i\omega(r_-^2 + a^2) - 2iam), \quad (3.8c)$$

$$\delta = 2\omega r_x (\omega(r_- + r_+) + is), \quad (3.8d)$$

$$\eta = 2is\omega r_+ - \frac{1}{2}s^2 - s - \hat{\lambda} - 2r_x^{-2}(\omega r_m - am)(\omega \hat{r}_0 - am). \quad (3.8e)$$

where $r_x = r_- - r_+$, $\hat{r}_0 = a^2 + 2r_-r_+ - r_+^2$, and $r_m = r_+^2 + a^2$. A more detailed derivation of the general solution (3.5) of the homogeneous Teukolsky equation can be seen in our previous work[60]. However, this derivation did not include the ingoing wave and outgoing wave solution for the Kerr spacetime, and their asymptotic amplitudes. Next, we will present the analytical expressions for these solutions.

The selection of the general solution (3.5) is advantageous in constructing the solutions that satisfy the normalized boundary conditions of the pure ingoing wave $R_{\ell\omega}^{\text{in}}(r)$ at the horizon and the

pure outgoing wave $R_{\ell\omega}^{\text{up}}(r)$ at infinity. Such as

$$R_{\ell m \omega}^{\text{in}} \rightarrow \begin{cases} \Delta^{-s} e^{-iPr^*}, & r \rightarrow r_{\text{H}}, \\ B_{\ell m \omega}^{\text{ref}} r^{1-2s} e^{i\omega r^*} + B_{\ell m \omega}^{\text{inc}} r^{-1} e^{-i\omega r^*}, & r \rightarrow +\infty, \end{cases} \quad (3.9)$$

$$R_{\ell m \omega}^{\text{up}} \rightarrow \begin{cases} C_{\ell m \omega}^{\text{up}} e^{iPr^*} + C_{\ell m \omega}^{\text{ref}} \Delta^{-s} e^{-iPr^*}, & r \rightarrow r_{\text{H}}, \\ r^{1-2s} e^{i\omega r^*}, & r \rightarrow +\infty, \end{cases} \quad (3.10)$$

where $P = \omega - m\Omega_{\text{H}}$ and $\Omega_{\text{H}} = \frac{a}{2Mr_+}$. Here, r^* is the tortoise coordinate defined by

$$r^* = r + \frac{2Mr_+}{r_+ - r_-} \ln \frac{r - r_+}{2M} - \frac{2Mr_-}{r_+ - r_-} \ln \frac{r - r_-}{2M}. \quad (3.11)$$

To construct two solutions $R_{\ell m \omega}^{\text{in,up}}$ satisfying the boundary conditions, only the coefficients C_1 and C_2 in the general solution (3.5) are required. Prior to undertaking this task, it becomes imperative to determine the asymptotic expressions of the confluent Heun function in the vicinity of the horizon and at infinity, respectively.

Expanding the confluent Heun function in a sector around the irregular singular point at event horizon $x = 0$ and infinity $x = \infty$, the asymptotic behavior at infinity can be expressed as:

$$\lim_{x \rightarrow 0} \text{HeunC}(\alpha, \beta, \gamma, \delta, \eta; x) = 1, \quad (3.12a)$$

$$\lim_{|x| \rightarrow \infty} \text{HeunC}(\alpha, \beta, \gamma, \delta, \eta; x) \rightarrow D_{\odot}^{\beta} x^{-\frac{\beta+\gamma+2}{2}-\frac{\delta}{\alpha}} + D_{\otimes}^{\beta} e^{-\alpha x} x^{-\frac{\beta+\gamma+2}{2}+\frac{\delta}{\alpha}}, \quad (3.12b)$$

where D_{\otimes}^{β} and D_{\odot}^{β} are constants, and their analytical expressions is shown in Appendix B.

Using the asymptotic properties (3.12) of the confluent Heun function and the boundary conditions (3.9) of the ingoing wave, we can construct the ingoing wave solution. The ingoing wave solution at the horizon has purely ingoing property, which imply $C_2^{\text{in}} = 0$. Thus, the ingoing wave solution $R_{\ell m \omega}^{\text{in}}$ is given by

$$R_{\ell m \omega}^{\text{in}} = S_0^{\beta}(x) \text{HeunC}(\alpha, \beta, \gamma, \delta, \eta; x). \quad (3.13)$$

By utilizing the asymptotic behavior (3.9) of the solution $R_{\ell m \omega}^{\text{in}}$ as $r \rightarrow \infty$, we derive analytic expressions for the asymptotic amplitudes $B_{\ell m \omega}^{\text{inc}}$ and $B_{\ell m \omega}^{\text{ref}}$,

$$B_{\ell m \omega}^{\text{inc}} = (-r_x)^{1-2s+i\frac{ma}{r_+}} (2M)^{-i\frac{ma}{r_+}} e^{i\frac{ma}{2M}} (-1)^{-\frac{\beta+\gamma+2}{2}-\frac{\delta}{\alpha}} D_{\odot}^{\beta}, \quad (3.14a)$$

$$B_{\ell m \omega}^{\text{ref}} = (-r_x) \left(-\frac{2M}{r_x} \right)^{2iM(P+\omega)} e^{-i(P+\omega)r_+} (-1)^{-\frac{\beta+\gamma+2}{2}+\frac{\delta}{\alpha}} D_{\otimes}^{\beta}. \quad (3.14b)$$

Similarly, according to the asymptotic properties (3.12) of the HeunC function and the boundary conditions (3.10) of the outgoing wave, we can construct the outgoing wave solution, can be given by

$$R_{\ell m \omega}^{\text{up}} = \left[(-1)^{\beta+1} \frac{D_{\odot}^{-\beta}}{D_{\otimes}^{\beta}} S_0^{\beta}(x) \text{HeunC}(\alpha, \beta, \gamma, \delta, \eta; x) + S_0^{-\beta}(x) \text{HeunC}(\alpha, -\beta, \gamma, \delta, \eta; x) \right]. \quad (3.15)$$

By utilizing the asymptotic behavior (3.10) of the solution $R_{\ell m \omega}^{\text{up}}$ as $r \rightarrow r_{\text{H}}$, we derive analytic expressions for the asymptotic amplitudes $C_{\ell m \omega}^{\text{ref}}$ and $C_{\ell m \omega}^{\text{up}}$,

$$C_{\ell m \omega}^{\text{ref}} = (-r_x)^{-1+2iM(P+\omega)} (2M)^{-2iM(P+\omega)} e^{i(P+\omega)r_+} (-1)^{2+\frac{\beta+\gamma}{2}-\frac{\delta}{\alpha}} \frac{D_{\odot}^{-\beta}}{D_{\odot}^{\beta}} \tilde{D}, \quad (3.16a)$$

$$C_{\ell m \omega}^{\text{up}} = (-r_x)^{-2s-1+i\frac{ma}{r_+}} (2M)^{-i\frac{ma}{r_+}} e^{i\frac{ma}{2M}} (-1)^{\frac{-\beta+\gamma+2}{2}-\frac{\delta}{\alpha}} \tilde{D}. \quad (3.16b)$$

with

$$\tilde{D} = \left(D_{\otimes}^{-\beta} - \frac{D_{\odot}^{-\beta}}{D_{\otimes}^{\beta}} D_{\otimes}^{\beta} \right)^{-1}.$$

The parameters $(\alpha, \beta, \gamma, \delta, \eta)$ of the confluent Heun function in this paper use the symbol of *Maple* software. In order to facilitate the reader to use other software for calculation, the conversion relationship of the parameters of the confluent Heun function between different software can be seen in Appendix C.

3.2 Radiative Fluxes

The separated radial function $R_{\ell m \omega}(r)$ has simple asymptotic behaviors that are only ingoing at the horizon and only outgoing at infinity.

$$R_{\ell m \omega}(r) \rightarrow \begin{cases} Z_{\ell m \omega}^{\infty} r^3 e^{i\omega r^*}, & r \rightarrow \infty, \\ Z_{\ell m \omega}^{\text{H}} \Delta e^{-iPr^*}, & r \rightarrow r_+. \end{cases} \quad (3.17)$$

The amplitudes $Z_{\ell m \omega}^{\infty, \text{H}}$ are obtained by the Green's function method, that is, by integrating homogeneous solutions $R_{\ell m \omega}^{\text{in, up}}$ and the source term $T_{\ell m \omega}$ from the separated radial Teukolsky equation. Further detailed discussion of non-rotating BHs can be found in Ref. [60]. The integral formula of the amplitudes $Z_{\ell m \omega}^{\infty, \text{H}}$ can be written in the following form

$$Z_{\ell m \omega}^{\infty, \text{H}} = \int_{-\infty}^{\infty} d\tau e^{i\omega[t(\tau)-t_0]} e^{-im\phi(\tau)} \mathcal{I}_{\ell m \omega}^{\infty, \text{H}}[r(\tau), \theta(\tau)]. \quad (3.18)$$

where the integration variable τ is proper time along the geodesic.

The function $\mathcal{I}_{\ell m \omega}^{\infty, \text{H}}(r, \theta)$ is discussed in our previous work [60]; schematically, it is a Green's function used to obtain ingoing wave and outgoing wave solutions $R_{\ell m \omega}^{\text{in, up}}$ of the Teukolsky equation, multiplied by this equation's source term.

$$\mathcal{I}_{\ell m \omega}^{\infty, \text{H}} = \frac{1}{W_{\text{C}}} \left[(A_{nn0} + A_{\bar{m}m0} + A_{\bar{m}\bar{m}0}) R_{\ell m \omega}^{\text{in, up}} - (A_{\bar{m}n1} + A_{\bar{m}\bar{m}1}) \left(R_{\ell m \omega}^{\text{in, up}} \right)' + A_{\bar{m}\bar{m}2} \left(R_{\ell m \omega}^{\text{in, up}} \right)'' \right], \quad (3.19)$$

where $'$ denotes $\partial/\partial r$, and W_{C} is the conserved Wronskian, that is

$$W_{\text{C}} = R_{\ell m \omega}^{\text{up}} \frac{d}{dr^*} R_{\ell m \omega}^{\text{in}} - R_{\ell m \omega}^{\text{in}} \frac{d}{dr^*} R_{\ell m \omega}^{\text{up}} = 2i\omega B_{\ell m \omega}^{\text{inc}}. \quad (3.20)$$

and A_{nn0} and other terms are given in Refs. [20, 63]. From Eqs. (2.7) and (2.8), we can change integration variable from proper time τ to Mino time λ for Eq. (3.18).

$$Z_{\ell m \omega}^{\infty, \text{H}} = e^{-im\phi_0} \int_{-\infty}^{\infty} d\lambda e^{i(\omega\Upsilon_{\tau} - m\Upsilon_{\phi})\lambda} \mathcal{J}_{\ell m \omega}^{\infty, \text{H}}[r(\lambda), \theta(\lambda)], \quad (3.21)$$

where we have introduced

$$J_{lm\omega}^{\infty,H}(r, \theta) = (r^2 + a^2 \cos^2 \theta) \mathcal{I}_{lm\omega}^{\infty,H}(r, \theta) e^{i\omega[\Delta t_r(r) + \Delta t_\theta(\theta)]} e^{-im[\Delta \phi_r(r) + \Delta \phi_\theta(\theta)]}. \quad (3.22)$$

Due to the periodicity of r and θ directions of orbital motions with respect to Mino time, the function $J_{lm\omega}^{\infty,H}$ can be written as a double Fourier series [48]:

$$J_{lm\omega}^{\infty,H} = \sum_{k=-\infty}^{\infty} \sum_{n=-\infty}^{\infty} J_{\ell m kn}^{\infty,H} e^{-i(k\Upsilon_\theta + n\Upsilon_r)\lambda}, \quad (3.23)$$

where

$$J_{\ell m kn}^{\infty,H} = \frac{1}{\Lambda_r \Lambda_\theta} \int_0^{\Lambda_r} d\lambda_r e^{in\Upsilon_r \lambda_r} \int_0^{\Lambda_\theta} d\lambda_\theta e^{ik\Upsilon_\theta \lambda_\theta} J_{lm\omega}^{\infty,H}[r(\lambda_r), \theta(\lambda_\theta)]. \quad (3.24)$$

From Eqs. (2.14), (3.21), (3.23) and (3.24), we find that

$$Z_{lm\omega}^{\infty,H} = \sum_{k=-\infty}^{\infty} \sum_{n=-\infty}^{\infty} Z_{\ell m kn}^{\infty,H} \delta(\omega - \omega_{mkn}), \quad (3.25)$$

where

$$\omega_{mkn} = m\Omega_\phi + k\Omega_\theta + n\Omega_r \quad (3.26)$$

and

$$Z_{\ell m kn}^{\infty,H} = e^{-im\phi_0} J_{\ell m kn}^{\infty,H} / \Upsilon_t. \quad (3.27)$$

These coefficients have the symmetry

$$Z_{\ell, -m, -k, -n}^{\infty,H} = (-1)^{(\ell+k)} \bar{Z}_{\ell m kn}^{\infty,H}, \quad (3.28)$$

where overbar denotes complex conjugation.

In the actual calculation of the amplitudes $Z_{\ell m kn}^{\infty,H}$, we can utilize the symmetry (3.28) of the amplitudes $Z_{\ell m kn}^{\infty,H}$: first calculate the amplitudes $Z_{\ell m kn}^{\infty,H}$ for all ℓ , all m , all k , and $n \geq 0$, to calculate the half of the modal amplitudes, and then use Eq. (3.28) to obtain the other half of the results. This has the advantage of reducing the amount of computation roughly in half. The efficient calculation of the amplitudes $Z_{\ell m kn}^{\infty,H}$ facilitates us to quickly obtain the GW radiative fluxes and the inspiral waveform of adiabatic evolution.

The phase of $Z_{\ell m kn}^{\infty,H}$ depends on the values of $(\lambda_{r0}, \lambda_{\theta0})$, and these values depend on the initial anomaly angles $(\chi_{r0}, \chi_{\theta0})$. We use $\check{Z}_{\ell m kn}^{\infty,H}$ to represent the amplitudes $Z_{\ell m kn}^{\infty,H}$ of the fiducial geodesic. Then the new expression of $Z_{\ell m \omega}^{\infty,H}$ can also be written as the phase factor multiplied by the fiducial geodesic value $Z_{\ell m \omega}^{\infty,H}$,

$$Z_{\ell m kn}^{\infty,H} = e^{i\xi_{mkn}} \check{Z}_{\ell m kn}^{\infty,H}, \quad (3.29)$$

where the correcting phase is

$$\xi_{mkn} = k\Upsilon_\theta \lambda_{\theta0} + n\Upsilon_r \lambda_{r0} + m \left[\Delta \check{\phi}_r(-\lambda_{r0}) + \Delta \check{\phi}_\theta(-\lambda_{\theta0}) - \phi_0 \right] - \omega_{mkn} \left[\Delta \check{t}_r(-\lambda_{r0}) + \Delta \check{t}_\theta(-\lambda_{\theta0}) \right]. \quad (3.30)$$

The initial condition affects these amplitudes only through the phase factor ξ_{mkn} . This fact means that we only need to calculate and store the quantities on the fiducial geodesics. By using Eq. (3.30), then we can easily convert these results to any initial conditions. This greatly reduces

the amount of computation required to cover physically important EMRI systems. Therefore, ξ_{mkn} can be rewritten in the following form [48]

$$\xi_{mkn} = m\xi_{100} + k\xi_{010} + n\xi_{001}. \quad (3.31)$$

For each orbit one need only compute $(\xi_{100}, \xi_{010}, \xi_{001})$ to know the phases for all (ℓ, m, k, n) .

Next, it is very simple to obtain the radiative fluxes of energy and angular momentum. It is only necessary to multiply the amplitudes of each mode by its weight coefficient and then sum it.

$$\left\langle \frac{dE}{dt} \right\rangle = \sum_{\ell mkn} \frac{1}{4\pi\omega_{mkn}^2} \left(|Z_{\ell mkn}^\infty|^2 + \alpha_{\ell m\omega} |Z_{\ell mkn}^H|^2 \right), \quad (3.32)$$

$$\left\langle \frac{dL_z}{dt} \right\rangle = \sum_{\ell mkn} \frac{m}{4\pi\omega_{mkn}^3} \left(|Z_{\ell mkn}^\infty|^2 + \alpha_{\ell m\omega} |Z_{\ell mkn}^H|^2 \right), \quad (3.33)$$

where $\langle \dots \rangle$ represents the time average. And

$$\alpha_{\ell m\omega} = \frac{256(2Mr_+)^5 P(P^2 + 4\tilde{\epsilon}^2)(P^2 + 16\tilde{\epsilon}^2)\omega^3}{|C|^2}, \quad (3.34)$$

$$|C|^2 = \left[(\lambda + 2)^2 + 4a\omega m - 4a^2\omega^2 \right] \left[\lambda^2 + 36a\omega m - 36a^2\omega^2 \right] + (2\lambda + 3)(96a^2\omega^2 - 48a\omega m) + 144\omega^2(M^2 - a^2). \quad (3.35)$$

with $\tilde{\epsilon} = \sqrt{M^2 - a^2}/(4Mr_+)$.

For simplicity, we set some abbreviations:

$$\{ \langle dE/dt \rangle, \langle dL_z/dt \rangle \} = \{ \dot{E}, \dot{L}_z \}, \quad (3.36)$$

$$\sum_{\ell mkn} \rightarrow \sum_{\ell=2}^{\infty} \sum_{m=1}^{\ell} \sum_{k=-\infty}^{\infty} \sum_{n=-\infty}^{\infty}. \quad (3.37)$$

When the object is in a Kerr geodesic orbit, it can be characterized (under initial conditions) by the orbital integrals E and L_z . The results of $\{ \dot{E}, \dot{L}_z \}$ have been known for a long time [22]; It can be realized from Eq. (3.32) and (3.33) that these quantities can be two regular fields, which are regular at the event horizon and infinity, respectively. The former can be calculated by the gravitational radiation at infinity. Calculating the gravitational radiation at down-horizon is a bit tricky; you have to calculate how tidal stresses shear generators of the horizon, increase its surface area (or entropy), and then apply the first law of BH dynamics to infer changes in the mass and spin of BHs.

4 Comparisons with other methods

In our previous papers [60], it has been demonstrated that the energy flux calculation of the HeunC method is much better than the results of any high-order post-Newtonian expansion [74] and numerical MST method [75–77] for a particle in circular orbits around a non-rotating BH. In this section, we numerically simulate the motion of the test particles around a rotating BH along a

generic orbit, and compare the computational performance of other methods [75]. For the calculation of energy fluxes in the BHPToolkit [75], the numerical integration method³ is used to calculate the homogeneous Teukolsky equation, and the full MST method is used to calculate the asymptotic amplitudes $B_{\ell m \omega}^{\text{inc,ref}}$ and $C_{\ell m \omega}^{\text{inc,up}}$. Compared with the MST method, this method of combining MST and numerical integration can calculate Eq. (3.21) more efficiently. We label this method as MST-NI method, and the exact solution in this paper is the results of the MST-NI method with the floating-point numbers $\mathbf{N} = 300$. Here, the floating-point numbers \mathbf{N} is ‘‘MachinePrecision’’ in Mathematica, which can affect the computational efficiency. The larger \mathbf{N} , the more calculation time is required. In our tables and figures, Δ_E is the relative error.

Table 1. Computational cost of GW energy fluxes for different Orbits.

Circular Orbit [♣]				Spherical Orbit [◇]				Eccentric Orbit [▽]				Generic Orbit [♠]			
a	Δ_E	HeunC	MST	x_I	Δ_E	HeunC	MST	e	Δ_E	HeunC	MST	e	Δ_E	HeunC	MST
0.1	10^{-20}	34	38	0.1	10^{-20}	34	39	0.1	10^{-20}	32	44	0.1	10^{-20}	32	43
	10^{-30}	44	56		10^{-30}	44	61		10^{-30}	42	64		10^{-30}	42	63
0.3	10^{-20}	36	38	0.3	10^{-20}	33	39	0.3	10^{-20}	35	44	0.3	10^{-20}	31	43
	10^{-30}	45	57		10^{-30}	43	59		10^{-30}	42	64		10^{-30}	41	62
0.5	10^{-20}	38	38	0.5	10^{-20}	33	39	0.5	10^{-20}	36	44	0.5	10^{-20}	32	43
	10^{-30}	48	57		10^{-30}	44	59		10^{-30}	42	65		10^{-30}	42	63
0.7	10^{-20}	43	43	0.7	10^{-20}	34	39	0.7	10^{-20}	35	42	0.7	10^{-20}	37	44
	10^{-30}	53	57		10^{-30}	44	60		10^{-30}	44	62		10^{-30}	46	64
0.9	10^{-20}	53	54	0.9	10^{-20}	34	40	0.9	10^{-20}	44	44	0.9	10^{-20}	39	46
	10^{-30}	64	78		10^{-30}	44	61		10^{-30}	49	63		10^{-30}	47	68

[♣] The parameter of the circular orbit at the innermost stable circular orbit (ISCO) $p_{\text{ISCO}} = 6M$ is $\ell_{\text{max}} = 6$.

[◇] The parameters of the spherical orbit at $p = 10M$ are $a = 0.9, e = 0, \ell_{\text{max}} = 6, 1 \leq n \leq 5$.

[▽] The parameters of the eccentric orbit at $p = 10M$ are $a = 0.9, \theta_{\text{inc}} = 0, \ell_{\text{max}} = 5, 1 \leq k \leq 3$.

[♠] The parameters of the generic orbit at $p = 10M$ are $a = 0.9, x_I = 0.1, \ell_{\text{max}} = 4, 1 \leq n \leq 3, 1 \leq k \leq 3$.

To generate the data grids of energy flux, it is necessary to calculate the energy flux corresponding to the four orbital parameters (a, p, e, x_I). The data grid of energy flux is stored, which is an important database to facilitate the construction of inspiral waveforms with any mass ratio. It is estimated that 50% of all observable EMRIs will have eccentricities $e > 0.2$ as they are close to the final stable orbit [47, 79, 80]. Most EMRI events have large initial eccentricity, and the energy flux with large eccentricity will lose calculation accuracy and efficiency for frequency-domain methods of the mode-sum regularization [16]. In this section, we are more concerned about the accuracy of radiative fluxes in the large eccentricity, high spin, and strong-field regions. We give the relative errors of radiative fluxes corresponding to the four orbits of the three methods in Table 1. In the case of large spin, we draw the error changes of radiative fluxes in the circular orbit and the spherical orbit respectively in Figures 1 and 2. From these numerical comparisons, we can see that the accuracy of our method is better than that of the MST-NI method in the calculation of high

³In Refs. [75, 78], the Teukolsky equation is first transformed into Sasaki-Nakamura equation, and then the numerical integration method is used to solve this equation according to the specific boundary conditions of the Sasaki-Nakamura equation. This method cannot solve the asymptotic amplitudes $B_{\ell m \omega}^{\text{inc,ref}}$ and $C_{\ell m \omega}^{\text{inc,up}}$ of the homogeneous Teukolsky equation.

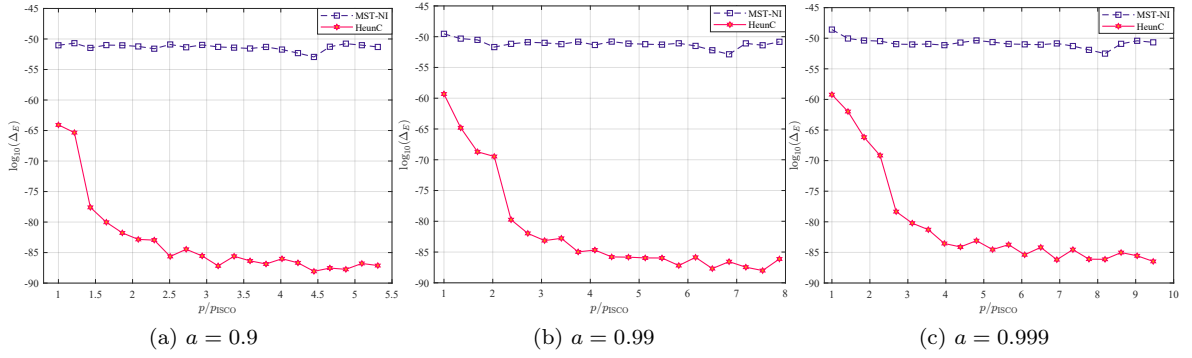


Figure 1. Logarithmic relative errors of radiative fluxes ($\ell_{\max} = 6$) of circular Orbits at $p = [p_{\text{ISCO}}, p_{\text{ISCO}} + 10M]$ with large spins $a = \{0.9, 0.99, 0.999\}$ and $\mathbf{N} = 100$.

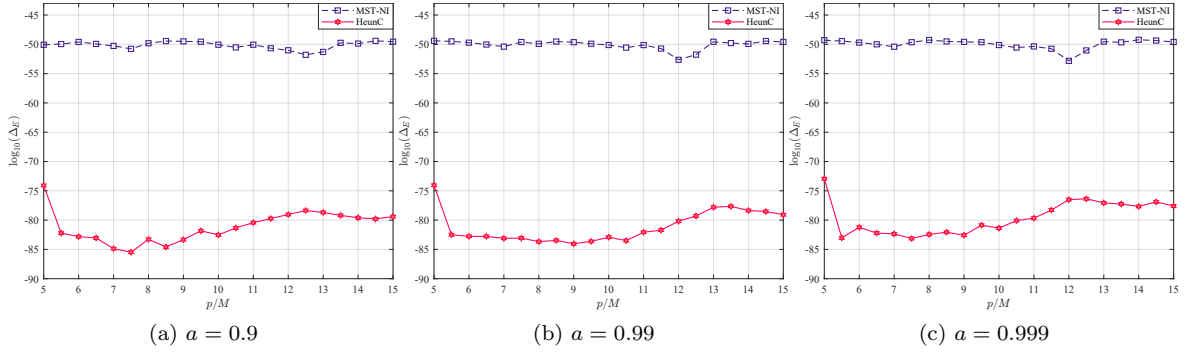


Figure 2. Logarithmic relative errors of radiative fluxes ($\ell_{\max} = 6$ and $1 \leq k \leq 5$) of spherical orbits ($x_I = 0.9$) at $p = [5M, 15M]$ with large spins $a = \{0.9, 0.99, 0.999\}$ and $\mathbf{N} = 100$.

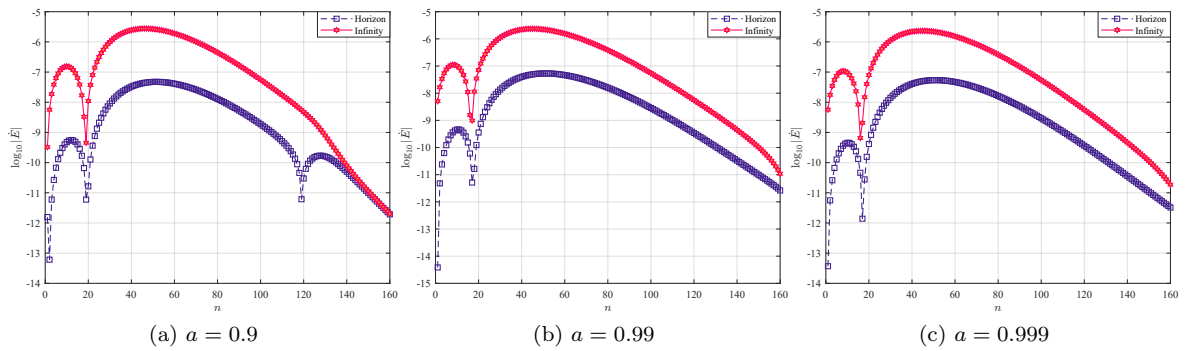
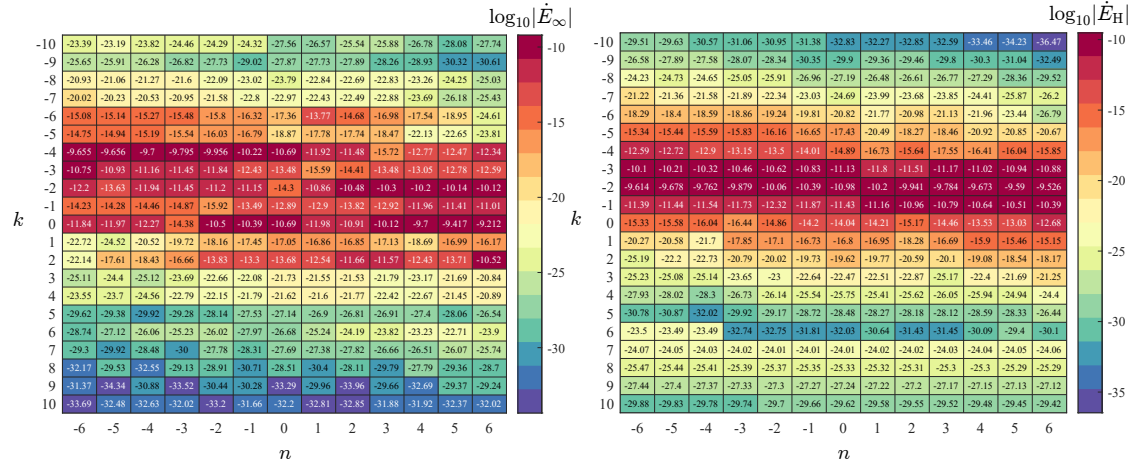
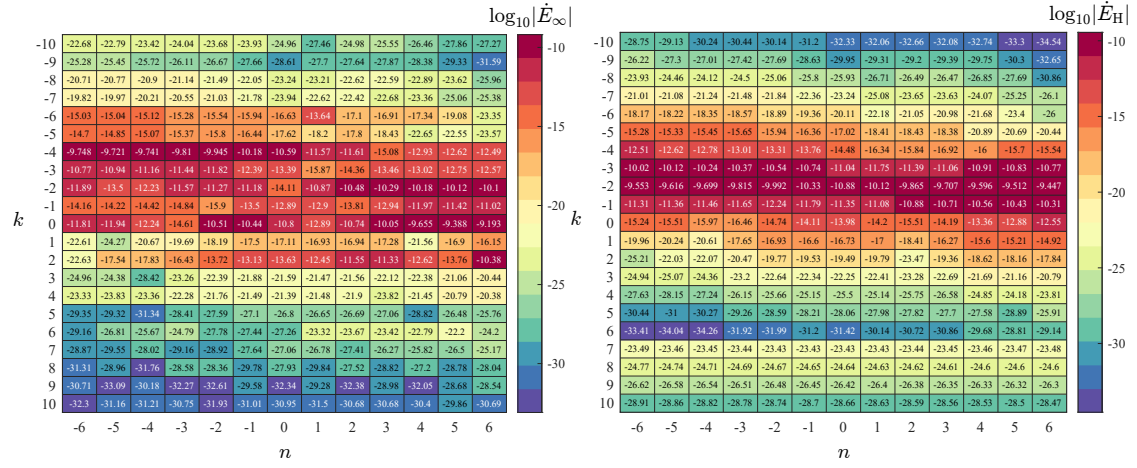


Figure 3. Modal radiative fluxes ($\ell = m = 2$) through the horizon and at infinity for the equatorial eccentric orbit ($e = 0.9$) at $p = 6M$ with large spins $a = \{0.9, 0.99, 0.999\}$ (To get the data quickly, we set $\mathbf{N} = 50$).



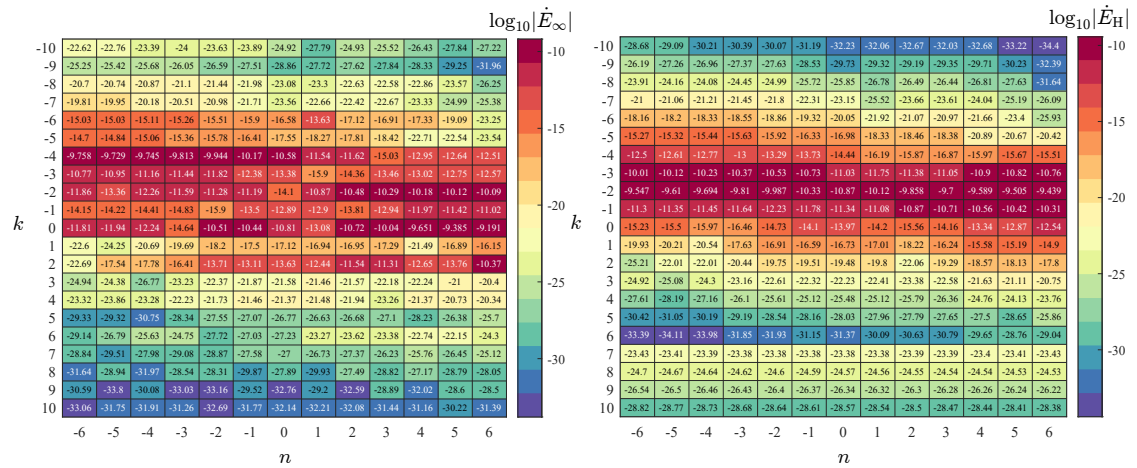
(a) Flux at infinity and $a = 0.9$

(b) Flux at horizon and $a = 0.9$



(c) Flux at infinity and $a = 0.99$

(d) Flux at horizon and $a = 0.99$



(e) Flux at infinity and $a = 0.999$

(f) Flux at horizon and $a = 0.999$

Figure 4. Modal radiative fluxes ($\ell = m = 2$) through the horizon and at infinity for the generic Orbit ($e = 0.9$ and $x_I = 0.1$) at $p = 10M$ with large spins $a = \{0.9, 0.99, 0.999\}$ and $N = 50$.

floating-point. For radiative fluxes of eccentric orbits, their values show a special behavior with the increase of the index n . They first increase to the peak value by oscillation, and then attenuate by oscillation [47, 52]. This behavior can be seen in Figure 3. Moreover, the results of the radiative fluxes of the generic orbital for large spins are shown in Figure 4.

From the above results, it can be seen that the HeunC method has excellent applicability and high precision, and can be used to calculate some extreme cases of general orbits: large eccentricity, higher spin, higher harmonic modes and strong-field regions. When calculating the radiative fluxes of a single higher harmonic mode, it is important to ensure higher floating-point accuracy. The total energy flux, which is obtained by summing thousands of (ℓ, m, k, n) modes, plays a crucial role in constructing waveform templates. Our method is capable of achieving higher accuracy using lower floating-point, which is advantageous for future efficiency enhancements.

5 Conclusion

In the previous study [60], the confluent Heun function was utilized to calculate the radiative fluxes resulting from the motion of test particles around a Schwarzschild BH in circular orbits. This paper expands our previous study to obtain the radiative fluxes generated by a particle in generic orbits around a near-extreme Kerr BH. This extension is effective for considering the gravitational radiation of binary star systems with varying mass ratios. Firstly, we discuss the geodesic dynamics of a point particle on generic orbits in the Kerr spacetime. Then, based on the confluent Heun function, we give the exact solution of Teukolsky equations for the Kerr spacetime. This solution is applied to obtain gravitational wave amplitude and radiative flux. Finally, our results are entirely satisfactory in comparison with the numerical methods. The findings are summarized in detail as follows:

1. From the numerical simulations, it can be seen that the HeunC method has excellent applicability and high precision, and can be used to calculate some extreme cases of general orbits: large eccentricity, higher spin, higher harmonic modes, and strong-field regions. Most frequency domain methods [16, 62, 81] frequently falter in accurately computing GW radiative fluxes in strong-field regions with highly eccentric generic orbits (with eccentricities $e \gtrsim 0.5$). Our method, although belonging to the frequency domain approach, overcomes these computational challenges.

2. The MST method has proven successful in EMRI waveform calculations, exhibiting incomparable computational accuracy and efficiency [48, 49, 56]. In the case of generic orbits, the calculation of higher harmonic modes requires high floating-point accuracy, because it involves the frequency calculation of four indexes (ℓ, m, k, n) . As our method undertakes higher floating-point calculations, its accuracy surpasses that of the MST-NI method and high-order post-Newtonian expansion due to the HeunC method's faster convergence speed⁴. When calculating the radiative fluxes of a single higher harmonic mode, it is important to ensure higher floating-point accuracy. The total energy flux, which is obtained by summing thousands of (ℓ, m, k, n) modes, plays a crucial role in constructing waveform templates. Our method is capable of achieving higher accuracy using lower floating-point numbers, which is advantageous for efficiency enhancements. This instills

⁴In our previous study [60], we have demonstrated in detail that the HeunC method exhibits a significantly faster convergence rate concerning floating-point numbers, compared to both the MST method, high-order post-Newtonian expansion, and numerical integration method.

confidence in us that the HeunC method will be used for the efficient calculation of GW waveforms in the future.

Acknowledgement

This work was supported by the Grant of NSFC Nos. 12035005 and 12122504, and National Key Research and Development Program of China No. 2020YFC2201400.

A Formulas for E , L_z , and Q

We provide formulas for the geodesic constants of the motion (E , L_z , Q) as functions of preferred parameters (p , e , x_I). The three geodesic constants of generic orbits can be written as

$$E = \sqrt{\frac{\kappa\rho + 2\varpi\sigma - 2\text{sgn}(x_I)\sqrt{\sigma(\sigma\varpi^2 + \rho\varpi\kappa - \eta\kappa^2)}}{\rho^2 + 4\eta\sigma}}, \quad (\text{A.1})$$

$$L_z = -\frac{g(r_a)E - \sqrt{g(r_a)^2 + h(r_a)f(r_a)E^2 - h(r_a)d(r_a)}}{h(r_a)}, \quad (\text{A.2})$$

$$Q = (1 - x_I^2) \left[a^2(1 - E^2) + \left(\frac{L_z}{x_I} \right)^2 \right], \quad (\text{A.3})$$

where

$$\kappa = d(r_a)h(r_p) - d(r_p)h(r_a), \quad (\text{A.4})$$

$$\varpi = d(r_a)g(r_p) - d(r_p)g(r_a), \quad (\text{A.5})$$

$$\rho = f(r_a)h(r_p) - f(r_p)h(r_a), \quad (\text{A.6})$$

$$\eta = f(r_a)g(r_p) - f(r_p)g(r_a), \quad (\text{A.7})$$

$$\sigma = g(r_a)h(r_p) - g(r_p)h(r_a), \quad (\text{A.8})$$

and

$$d(r) = \Delta(r)[r^2 + a^2(1 - x_I^2)], \quad (\text{A.9})$$

$$f(r) = r^4 + a^2[r(r + 2M) + (1 - x_I^2)\Delta(r)], \quad (\text{A.10})$$

$$g(r) = 2aMr, \quad (\text{A.11})$$

$$h(r) = r(r - 2M) + \frac{(1 - x_I^2)\Delta(r)}{x_I^2}, \quad (\text{A.12})$$

where $r_a = p/(1 - e)$ and $r_p = p/(1 + e)$ are the coordinate radius of the orbit's apoapsis and periapsis, respectively.

More details of these formulas can be seen in Refs. [61, 62]. In addition, we utilized some Hughes's adjustments [48] for the formula: ϖ replaces ϵ in Refs. [61, 62] to avoid the symbol conflict with $\epsilon = \sqrt{M^2 - a^2}/2Mr_+$ and the very similar $\varepsilon \equiv \mu/M$.

B Asymptotic Formula of HeunC Function at Infinity

In our previous study [60], we derive the asymptotic analytic expression of the confluent Heun function at infinity. Bonelli et al. solved the connection problem of Heun class functions [82]. By using the connection formulae of $x \in [0, 1]$ and $x \in [1, \infty]$ of the confluent Heun function derived by them, the connection formulae of $x \in [0, \infty]$ can be applied to calculate the HeunC value as x tends to infinity. Our analytic expression can also be used to calculate the HeunC value as $x \rightarrow \infty$, and it also contains the amplitude of some physical information. We provide the asymptotic expression of confluent Heun function $\mathbb{H} = \text{HeunC}(\alpha, \beta, \gamma, \delta, \eta; x)$ at infinity as follows

$$\lim_{|x| \rightarrow \infty} \mathbb{H}(x) = D_{\odot}^{\beta} x^{-\frac{\beta+\gamma+2}{2}-\frac{\delta}{\alpha}} + D_{\otimes}^{\beta} e^{-\alpha x} x^{-\frac{\beta+\gamma+2}{2}+\frac{\delta}{\alpha}}. \quad (\text{B.1})$$

Then, the constants D_{\odot}^{β} and D_{\otimes}^{β} are given by

$$D_{\odot}^{\beta} = \Xi_{n,\nu}^{\beta} D_{\odot,n,\nu}^{\beta} + e^{-i\pi(\nu+\frac{1}{2})} \frac{\sin \pi(\nu+\frac{\delta}{\alpha})}{\sin \pi(\nu-\frac{\delta}{\alpha})} \Xi_{-n,-\nu-1}^{\beta} D_{\odot,-n,-\nu-1}^{\beta}, \quad (\text{B.2})$$

$$D_{\otimes}^{\beta} = \Xi_{n,\nu}^{\beta} D_{\otimes,n,\nu}^{\beta} + e^{i\pi(\nu+\frac{1}{2})} \Xi_{-n,-\nu-1}^{\beta} D_{\otimes,-n,-\nu-1}^{\beta}, \quad (\text{B.3})$$

with

$$D_{\odot,n,\nu}^{\beta} = (-1)^{\frac{\gamma+\beta+2}{2}+\frac{\delta}{\alpha}} \left(\frac{\alpha}{2}\right)^{\tau} \left(-\frac{i\alpha}{2}\right)^{-\frac{\gamma+\beta+2}{2}-\frac{\delta}{\alpha}} e^{-\frac{i\pi\tau+\alpha}{2}} 2^{-1-\frac{\delta}{\alpha}} e^{\frac{i\pi}{2}(\nu+1+\frac{\delta}{\alpha})} \Xi_{n,\nu}^{\beta} \frac{\Gamma(\nu+1+\frac{\delta}{\alpha})}{\Gamma(\nu+1-\frac{\delta}{\alpha})}, \quad (\text{B.4})$$

$$D_{\otimes,n,\nu}^{\beta} = (-1)^{\frac{\gamma+\beta+2}{2}-\frac{\delta}{\alpha}} \left(\frac{\alpha}{2}\right)^{\tau} \left(-\frac{i\alpha}{2}\right)^{-\frac{\gamma+\beta+2}{2}+\frac{\delta}{\alpha}} e^{-\frac{i\pi\tau-\alpha}{2}} \Xi_{n,\nu}^{\beta} \frac{2^{-1+\frac{\delta}{\alpha}} e^{-\frac{i\pi}{2}(\nu+1-\frac{\delta}{\alpha})}}{\sum_{n=-\infty}^{+\infty} f_n^{\nu}} \times \left(\sum_{n=-\infty}^{+\infty} (-1)^n \frac{(\nu+1-\frac{\delta}{\alpha})_n}{(\nu+1+\frac{\delta}{\alpha})_n} f_n^{\nu} \right). \quad (\text{B.5})$$

and

$$\Xi_{n,\nu}^{\beta} = \frac{2^{-\nu(\frac{\alpha}{2})^{-\tau}} e^{\frac{i\pi\tau+\alpha}{2}} \Gamma(\beta+1)\Gamma(2\nu+2)}{\Gamma(\nu+1+\frac{\delta}{\alpha})\Gamma(\nu+1-\frac{\beta+\gamma}{2})\Gamma(\nu+1+\frac{\gamma-\beta}{2})} \times \left(\sum_{n=-\infty}^0 \frac{(-1)^n (\nu+1-\frac{\delta}{\alpha})_n}{(-n)!(2\nu+2)_n (\nu+1+\frac{\delta}{\alpha})_n} f_n^{\nu} \right)^{-1} \times \left(\sum_{n=0}^{\infty} (-1)^n \frac{\Gamma(n+2\nu+1)\Gamma(n+\nu+1+\frac{\gamma-\beta}{2})\Gamma(n+\nu+1-\frac{\beta+\gamma}{2})}{(n!)\Gamma(n+\nu+1+\frac{\beta-\gamma}{2})\Gamma(n+\nu+1+\frac{\beta+\gamma}{2})} f_n^{\nu} \right).$$

where $\tau = \frac{1}{4}(3\beta + \gamma + \frac{2\delta}{\alpha})$, and f_n^{ν} satisfy the following three-term recurrence relation,

$$\hat{\alpha}_n f_{n+1}^{\nu} + \hat{\beta}_n f_n^{\nu} + \hat{\gamma}_n f_{n-1}^{\nu} = 0, \quad (\text{B.7})$$

where

$$\hat{\alpha}_n = \frac{(2n + 2\nu + 2 - \beta + \gamma)}{8(n + \nu + 1)(2n + 2\nu + 3)} (an + \alpha\nu + \alpha - \delta)(2n + 2\nu + 2 - \gamma - \beta), \quad (\text{B.8a})$$

$$\hat{\beta}_n = \eta + \frac{\delta}{2} - \frac{\beta^2}{4} - \frac{\gamma^2}{4} + (n + \nu)(n + \nu + 1) + \frac{\delta(\gamma + \beta)(\beta - \gamma)}{8(n + \nu)(n + \nu + 1)}, \quad (\text{B.8b})$$

$$\hat{\gamma}_n = -\frac{(2n + 2\nu + \beta - \gamma)}{8(n + \nu)(2n + 2\nu - 1)} (an + \alpha\nu + \delta)(2n + 2\nu + \gamma + \beta). \quad (\text{B.8c})$$

The phase parameter ν , also known as the renormalized angular momentum, may be obtained by solving a characteristic equation expressed as the sum of two infinite continued fractions.

$$\hat{\beta}_0 = \frac{\hat{\alpha}_{-1}\hat{\gamma}_0}{\hat{\beta}_{-1-}} - \frac{\hat{\alpha}_{-2}\hat{\gamma}_{-1}}{\hat{\beta}_{-2-}} - \frac{\hat{\alpha}_{-3}\hat{\gamma}_{-2}}{\hat{\beta}_{-3-}} + \dots + \frac{\hat{\alpha}_0\hat{\gamma}_1}{\hat{\beta}_{1-}} - \frac{\hat{\alpha}_1\hat{\gamma}_2}{\hat{\beta}_{2-}} - \frac{\hat{\alpha}_2\hat{\gamma}_3}{\hat{\beta}_{3-}} \dots \quad (\text{B.9})$$

C Parameters of HeunC Functions

Currently, three primary mathematical software packages offer numerical calculation capabilities for the confluent Heun function, as well as for its derivation and integration. Maple and Mathematica provide official built-in functions for these calculations, while the calculation code of MATLAB is provided by Motygin [83, 84].

For Maple software, the ODE of the confluent Heun function $\mathbb{H}_0^\beta(x) = \text{HeunC}(\alpha, \beta, \gamma, \delta, \eta; x)$ can be written as

$$\mathbb{H}'' - \frac{(-x^2\alpha + (-2 - \beta - \gamma + \alpha)x + 1 + \beta)}{x(x-1)}\mathbb{H}' - \left[\left((-2 - \beta - \gamma)\alpha - 2\delta \right)x + (\beta + 1)\alpha + (-\gamma - 1)\beta - \gamma - 2\eta \right] \frac{\mathbb{H}}{2x(x-1)} = 0. \quad (\text{C.1})$$

For MATLAB/Mathematica software, the ODE of the confluent Heun function can be written as

$$\mathbf{H}'' + \mathbf{H}' \left(\frac{\gamma_M}{x} + \frac{\delta_M}{x-1} + \epsilon_M \right) + \frac{(\alpha_M x - q_M)}{x(x-1)} \mathbf{H} = 0 \quad (\text{C.2})$$

where $\mathbf{H}(x) = \text{HeunC}(q_M, \alpha_M, \gamma_M, \delta_M, \epsilon_M; x)$.

The parameter relation between Eqs. (C.1) and (C.2) is as follows

$$q_M = \frac{1}{2}\alpha\beta - \frac{1}{2}\beta\gamma + \frac{1}{2}\alpha - \frac{1}{2}\beta - \eta - \frac{1}{2}\gamma, \quad (\text{C.3a})$$

$$\alpha_M = \frac{1}{2}\alpha\beta + \frac{1}{2}\alpha\gamma + \alpha + \delta, \quad (\text{C.3b})$$

$$\delta_M = \gamma + 1, \quad (\text{C.3c})$$

$$\epsilon_M = \alpha, \quad (\text{C.3d})$$

$$\gamma_M = \beta + 1. \quad (\text{C.3e})$$

References

- [1] LIGO SCIENTIFIC, VIRGO collaboration, *Improved analysis of GW150914 using a fully spin-precessing waveform Model*, *Phys. Rev. X* **6** (2016) 041014 [1606.01210].

- [2] LIGO SCIENTIFIC, VIRGO collaboration, *Binary Black Hole Mergers in the first Advanced LIGO Observing Run*, *Phys. Rev. X* **6** (2016) 041015 [[1606.04856](#)].
- [3] LIGO SCIENTIFIC, VIRGO collaboration, *GWTC-1: A Gravitational-Wave Transient Catalog of Compact Binary Mergers Observed by LIGO and Virgo during the First and Second Observing Runs*, *Phys. Rev. X* **9** (2019) 031040 [[1811.12907](#)].
- [4] LIGO SCIENTIFIC, VIRGO collaboration, *GWTC-2: Compact Binary Coalescences Observed by LIGO and Virgo During the First Half of the Third Observing Run*, *Phys. Rev. X* **11** (2021) 021053 [[2010.14527](#)].
- [5] KAGRA, VIRGO, LIGO SCIENTIFIC collaboration, *Population of Merging Compact Binaries Inferred Using Gravitational Waves through GWTC-3*, *Phys. Rev. X* **13** (2023) 011048 [[2111.03634](#)].
- [6] LISA collaboration, *Laser Interferometer Space Antenna*, [1702.00786](#).
- [7] LISA CONSORTIUM WAVEFORM WORKING GROUP collaboration, *Waveform Modelling for the Laser Interferometer Space Antenna*, [2311.01300](#).
- [8] TIANQIN collaboration, *TianQin: a space-borne gravitational wave detector*, *Class. Quant. Grav.* **33** (2016) 035010 [[1512.02076](#)].
- [9] TIANQIN collaboration, *The TianQin project: current progress on science and technology*, *PTEP* **2021** (2021) 05A107 [[2008.10332](#)].
- [10] W.-H. Ruan, Z.-K. Guo, R.-G. Cai and Y.-Z. Zhang, *Taiji program: Gravitational-wave sources*, *Int. J. Mod. Phys. A* **35** (2020) 2050075 [[1807.09495](#)].
- [11] S. Babak, J. Gair, A. Sesana, E. Barausse, C.F. Sopuerta, C.P.L. Berry et al., *Science with the space-based interferometer LISA. V: Extreme mass-ratio inspirals*, *Phys. Rev. D* **95** (2017) 103012 [[1703.09722](#)].
- [12] Y. Mino, M. Sasaki and T. Tanaka, *Gravitational radiation reaction to a particle motion*, *Phys. Rev. D* **55** (1997) 3457 [[gr-qc/9606018](#)].
- [13] T.C. Quinn and R.M. Wald, *An Axiomatic approach to electromagnetic and gravitational radiation reaction of particles in curved space-time*, *Phys. Rev. D* **56** (1997) 3381 [[gr-qc/9610053](#)].
- [14] L. Barack, *Gravitational self force in extreme mass-ratio inspirals*, *Class. Quant. Grav.* **26** (2009) 213001 [[0908.1664](#)].
- [15] E. Poisson, A. Pound and I. Vega, *The Motion of point particles in curved spacetime*, *Living Rev. Rel.* **14** (2011) 7 [[1102.0529](#)].
- [16] B. Wardell, *Self-force: Computational Strategies*, *Fund. Theor. Phys.* **179** (2015) 487 [[1501.07322](#)].
- [17] A. Pound, *Motion of small objects in curved spacetimes: An introduction to gravitational self-force*, *Fund. Theor. Phys.* **179** (2015) 399 [[1506.06245](#)].
- [18] A. Pound and B. Wardell, *Black hole perturbation theory and gravitational self-force*, [2101.04592](#).
- [19] S.A. Teukolsky, *Rotating black holes - separable wave equations for gravitational and electromagnetic perturbations*, *Phys. Rev. Lett.* **29** (1972) 1114.
- [20] S.A. Teukolsky, *Perturbations of a rotating black hole. I. Fundamental equations for gravitational electromagnetic and neutrino field perturbations*, *Astrophys. J.* **185** (1973) 635.

- [21] W.H. Press and S.A. Teukolsky, *Perturbations of a Rotating Black Hole. II. Dynamical Stability of the Kerr Metric*, *Astrophys. J.* **185** (1973) 649.
- [22] S.A. Teukolsky and W.H. Press, *Perturbations of a rotating black hole. III - Interaction of the hole with gravitational and electromagnetic radiation*, *Astrophys. J.* **193** (1974) 443.
- [23] R.M. Wald, *On perturbations of a Kerr black hole*, *J. Math. Phys.* **14** (1973) 1453.
- [24] J.M. Cohen and L.S. Kegeles, *Electromagnetic fields in curved spaces - a constructive procedure*, *Phys. Rev. D* **10** (1974) 1070.
- [25] P.L. Chrzanowski, *Vector Potential and Metric Perturbations of a Rotating Black Hole*, *Phys. Rev. D* **11** (1975) 2042.
- [26] L.S. Kegeles and J.M. Cohen, *CONSTRUCTIVE PROCEDURE FOR PERTURBATIONS OF SPACE-TIMES*, *Phys. Rev. D* **19** (1979) 1641.
- [27] A. Ori, *Reconstruction of inhomogeneous metric perturbations and electromagnetic four potential in Kerr space-time*, *Phys. Rev. D* **67** (2003) 124010 [gr-qc/0207045].
- [28] A. Pound, C. Merlin and L. Barack, *Gravitational self-force from radiation-gauge metric perturbations*, *Phys. Rev. D* **89** (2014) 024009 [1310.1513].
- [29] T.S. Keidl, J.L. Friedman and A.G. Wiseman, *On finding fields and self-force in a gauge appropriate to separable wave equations*, *Phys. Rev. D* **75** (2007) 124009 [gr-qc/0611072].
- [30] T.S. Keidl, A.G. Shah, J.L. Friedman, D.-H. Kim and L.R. Price, *Gravitational Self-force in a Radiation Gauge*, *Phys. Rev. D* **82** (2010) 124012 [1004.2276].
- [31] A.G. Shah, T.S. Keidl, J.L. Friedman, D.-H. Kim and L.R. Price, *Conservative, gravitational self-force for a particle in circular orbit around a Schwarzschild black hole in a Radiation Gauge*, *Phys. Rev. D* **83** (2011) 064018 [1009.4876].
- [32] A.G. Shah, J.L. Friedman and T.S. Keidl, *EMRI corrections to the angular velocity and redshift factor of a mass in circular orbit about a Kerr black hole*, *Phys. Rev. D* **86** (2012) 084059 [1207.5595].
- [33] M. van de Meent and A.G. Shah, *Metric perturbations produced by eccentric equatorial orbits around a Kerr black hole*, *Phys. Rev. D* **92** (2015) 064025 [1506.04755].
- [34] M. van de Meent, *Self-force corrections to the periastron advance around a spinning black hole*, *Phys. Rev. Lett.* **118** (2017) 011101 [1610.03497].
- [35] M. van de Meent, *Gravitational self-force on generic bound geodesics in Kerr spacetime*, *Phys. Rev. D* **97** (2018) 104033 [1711.09607].
- [36] C. Merlin, A. Ori, L. Barack, A. Pound and M. van de Meent, *Completion of metric reconstruction for a particle orbiting a Kerr black hole*, *Phys. Rev. D* **94** (2016) 104066 [1609.01227].
- [37] M. van De Meent, *The mass and angular momentum of reconstructed metric perturbations*, *Class. Quant. Grav.* **34** (2017) 124003 [1702.00969].
- [38] T. Hinderer and E.E. Flanagan, *Two timescale analysis of extreme mass ratio inspirals in Kerr. I. Orbital Motion*, *Phys. Rev. D* **78** (2008) 064028 [0805.3337].
- [39] E.E. Flanagan and T. Hinderer, *Transient resonances in the inspirals of point particles into black holes*, *Phys. Rev. Lett.* **109** (2012) 071102 [1009.4923].
- [40] Y. Mino, *Perturbative approach to an orbital evolution around a supermassive black hole*, *Phys. Rev. D* **67** (2003) 084027 [gr-qc/0302075].

- [41] N. Sago, T. Tanaka, W. Hikida, K. Ganz and H. Nakano, *The Adiabatic evolution of orbital parameters in the Kerr spacetime*, *Prog. Theor. Phys.* **115** (2006) 873 [gr-qc/0511151].
- [42] T. Osburn, E. Forseth, C.R. Evans and S. Hopper, *Lorenz gauge gravitational self-force calculations of eccentric binaries using a frequency domain procedure*, *Phys. Rev. D* **90** (2014) 104031 [1409.4419].
- [43] M. Sasaki and T. Nakamura, *The regge-wheeler equation with sources for both even and odd parity perturbations of the schwarzschild geometry*, *Phys. Lett. A* **87** (1981) 85.
- [44] S.A. Hughes, *The Evolution of circular, nonequatorial orbits of Kerr black holes due to gravitational wave emission*, *Phys. Rev. D* **61** (2000) 084004 [gr-qc/9910091].
- [45] S.A. Hughes, *Evolution of circular, nonequatorial orbits of Kerr black holes due to gravitational wave emission. II. Inspiral trajectories and gravitational wave forms*, *Phys. Rev. D* **64** (2001) 064004 [gr-qc/0104041].
- [46] S. Drasco and S.A. Hughes, *Rotating black hole orbit functionals in the frequency domain*, *Phys. Rev. D* **69** (2004) 044015 [astro-ph/0308479].
- [47] S. Drasco and S.A. Hughes, *Gravitational wave snapshots of generic extreme mass ratio inspirals*, *Phys.Rev.D* **73** (2006) 024027 [gr-qc/0509101].
- [48] S.A. Hughes, N. Warburton, G. Khanna, A.J.K. Chua and M.L. Katz, *Adiabatic waveforms for extreme mass-ratio inspirals via multivoice decomposition in time and frequency*, *Phys. Rev. D* **103** (2021) 104014 [2102.02713].
- [49] V. Skoupy, G. Lukes-Gerakopoulos, L.V. Drummond and S.A. Hughes, *Asymptotic gravitational-wave fluxes from a spinning test body on generic orbits around a Kerr black hole*, *Phys. Rev. D* **108** (2023) 044041 [2303.16798].
- [50] L.V. Drummond and S.A. Hughes, *Precisely computing bound orbits of spinning bodies around black holes. I. General framework and results for nearly equatorial orbits*, *Phys. Rev. D* **105** (2022) 124040 [2201.13334].
- [51] L.V. Drummond and S.A. Hughes, *Precisely computing bound orbits of spinning bodies around black holes. II. Generic orbits*, *Phys. Rev. D* **105** (2022) 124041 [2201.13335].
- [52] R. Fujita, W. Hikida and H. Tagoshi, *An Efficient Numerical Method for Computing Gravitational Waves Induced by a Particle Moving on Eccentric Inclined Orbits around a Kerr Black Hole*, *Prog. Theor. Phys.* **121** (2009) 843 [0904.3810].
- [53] R. Fujita and W. Hikida, *Analytical solutions of bound timelike geodesic orbits in Kerr spacetime*, *Class. Quant. Grav.* **26** (2009) 135002 [0906.1420].
- [54] N. Sago and R. Fujita, *Calculation of radiation reaction effect on orbital parameters in Kerr spacetime*, *PTEP* **2015** (2015) 073E03 [1505.01600].
- [55] R. Fujita and M. Shibata, *Extreme mass ratio inspirals on the equatorial plane in the adiabatic order*, *Phys. Rev. D* **102** (2020) 064005 [2008.13554].
- [56] S. Isoyama, R. Fujita, A.J.K. Chua, H. Nakano, A. Pound and N. Sago, *Adiabatic Waveforms from Extreme-Mass-Ratio Inspirals: An Analytical Approach*, *Phys. Rev. Lett.* **128** (2022) 231101 [2111.05288].
- [57] B. Wardell, A. Pound, N. Warburton, J. Miller, L. Durkan and A. Le Tiec, *Gravitational Waveforms for Compact Binaries from Second-Order Self-Force Theory*, *Phys. Rev. Lett.* **130** (2023) 241402 [2112.12265].

- [58] C. Zhang, Y. Gong, D. Liang and B. Wang, *Gravitational waves from eccentric extreme mass-ratio inspirals as probes of scalar fields*, *JCAP* **06** (2023) 054 [2210.11121].
- [59] C. Zhang, H. Guo, Y. Gong and B. Wang, *Detecting vector charge with extreme mass ratio inspirals onto Kerr black holes*, *JCAP* **06** (2023) 020 [2301.05915].
- [60] C. Chen and J. Jing, *Radiation fluxes of gravitational, electromagnetic, and scalar perturbations in type-D black holes: an exact approach*, *JCAP* **11** (2023) 070 [2307.14616].
- [61] W. Schmidt, *Celestial mechanics in Kerr space-time*, *Class. Quant. Grav.* **19** (2002) 2743 [gr-qc/0202090].
- [62] M. van de Meent, *Analytic solutions for parallel transport along generic bound geodesics in Kerr spacetime*, *Class. Quant. Grav.* **37** (2020) 145007 [1906.05090].
- [63] M. Sasaki and H. Tagoshi, *Analytic black hole perturbation approach to gravitational radiation*, *Living Rev. Rel.* **6** (2003) 6 [gr-qc/0306120].
- [64] S. O’Sullivan and S.A. Hughes, *Strong-field tidal distortions of rotating black holes: Formalism and results for circular, equatorial orbits*, *Phys. Rev. D* **90** (2014) 124039 [1407.6983].
- [65] H. Tagoshi and M. Sasaki, *Post-Newtonian expansion of gravitational waves from a particle in circular orbit around a Schwarzschild black hole*, *Prog. Theor. Phys.* **92** (1994) 745 [gr-qc/9405062].
- [66] H. Tagoshi, M. Shibata, T. Tanaka and M. Sasaki, *Post-Newtonian expansion of gravitational waves from a particle in circular orbits around a rotating black hole: Up to $O(v^8)$ beyond the quadrupole formula*, *Phys. Rev. D* **54** (1996) 1439 [gr-qc/9603028].
- [67] T. Tanaka, H. Tagoshi and M. Sasaki, *Gravitational waves by a particle in circular orbits around a Schwarzschild black hole: 5.5 post-Newtonian formula*, *Prog. Theor. Phys.* **96** (1996) 1087 [gr-qc/9701050].
- [68] M. Shibata, M. Sasaki, H. Tagoshi and T. Tanaka, *Gravitational waves from a particle orbiting around a rotating black hole: Post-Newtonian expansion*, *Phys. Rev. D* **51** (1995) 1646 [gr-qc/9409054].
- [69] S. Mano, H. Suzuki and E. Takasugi, *Analytic solutions of the Regge-Wheeler equation and the post-Minkowskian expansion*, *Prog. Theor. Phys.* **96** (1996) 549 [gr-qc/9605057].
- [70] S. Mano, H. Suzuki and E. Takasugi, *Analytic solutions of the Teukolsky equation and their low frequency expansions*, *Prog. Theor. Phys.* **95** (1996) 1079 [gr-qc/9603020].
- [71] A. Ronveaux and F.M. Arscott, *Heun’s differential equations*, Oxford University Press (1995).
- [72] S. Slavyanov and W. Lay, *Special Functions: Unified Theory Based on Singularities*, Oxford University Press (2000).
- [73] F.W. Olver, D.W. Lozier, R.F. Boisvert and C.W. Clark, *NIST handbook of mathematical functions hardback and CD-ROM*, Cambridge university press (2010).
- [74] R. Fujita, *Gravitational Waves from a Particle in Circular Orbits around a Rotating Black Hole to the 11th Post-Newtonian Order*, *PTEP* **2015** (2015) 033E01 [1412.5689].
- [75] “Black Hole Perturbation Toolkit.” (bhptoolkit.org), 2023.
- [76] R. Fujita and H. Tagoshi, *New numerical methods to evaluate homogeneous solutions of the Teukolsky equation*, *Prog. Theor. Phys.* **112** (2004) 415 [gr-qc/0410018].

- [77] R. Fujita and H. Tagoshi, *New Numerical Methods to Evaluate Homogeneous Solutions of the Teukolsky Equation II. Solutions of the Continued Fraction Equation*, *Prog. Theor. Phys.* **113** (2005) 1165 [0904.3818].
- [78] S.E. Gralla, A.P. Porfyriadis and N. Warburton, *Particle on the Innermost Stable Circular Orbit of a Rapidly Spinning Black Hole*, *Phys. Rev. D* **92** (2015) 064029 [1506.08496].
- [79] L. Barack and C. Cutler, *LISA capture sources: Approximate waveforms, signal-to-noise ratios, and parameter estimation accuracy*, *Phys. Rev. D* **69** (2004) 082005 [gr-qc/0310125].
- [80] J.R. Gair, L. Barack, T. Creighton, C. Cutler, S.L. Larson, E.S. Phinney et al., *Event rate estimates for LISA extreme mass ratio capture sources*, *Class. Quant. Grav.* **21** (2004) S1595 [gr-qc/0405137].
- [81] J.L. Barton, D.J. Lazar, D.J. Kennefick, G. Khanna and L.M. Burko, *Computational Efficiency of Frequency and Time-Domain Calculations of Extreme Mass-Ratio Binaries: Equatorial Orbits*, *Phys. Rev. D* **78** (2008) 064042 [0804.1075].
- [82] G. Bonelli, C. Iossa, D. Panea Lichtig and A. Tanzini, *Irregular Liouville Correlators and Connection Formulae for Heun Functions*, *Commun. Math. Phys.* **397** (2023) 635 [2201.04491].
- [83] O.V. Motygin, *On numerical evaluation of the Heun functions*, in *2015 Days on Diffraction (DD)*, IEEE, may, 2015, DOI.
- [84] O.V. Motygin, *On evaluation of the confluent Heun functions*, in *2018 Days on Diffraction (DD)*, IEEE, 2018, DOI.